

Spin generation away from boundaries by nonlinear transport

Ilya G. Finkler, Hans-Andreas Engel, Emmanuel I. Rashba, Bertrand I. Halperin
Department of Physics, Harvard University, Cambridge, Massachusetts 02138

In several situations of interest, spin polarization may be generated far from the boundaries of a sample by nonlinear effects of an electric current, even when such a generation is forbidden by symmetry in the linear regime. We present an analytically solvable model where spin accumulation results from a combination of current gradients, nonlinearity, and cubic anisotropy. Further, we show that even with isotropic conductivity, nonlinear effects in a low symmetry geometry can generate spin polarization far away from boundaries. Finally, we find that drift from the boundaries results in spin polarization patterns that dominate in recent experiments on GaAs by Sih *et al.* [Phys. Rev. Lett. **97**, 096605 (2006)].

Spin polarization can be generated and manipulated in semiconductors by means of electric fields and spin-orbit coupling. A prominent example is the spin Hall effect,^{1,2,3,4,5,6,7,8,9} where a homogeneous electric current passing through a sample induces spin polarization $\mathbf{s}(\mathbf{r})$ near lateral edges, with opposite polarization at opposite edges. For rectangular homogeneous samples, this spin polarization falls off exponentially when moving away from the boundary on the length scale of the spin diffusion length L_s , so for samples of size $L > L_s$ no spin polarization due to the spin Hall effect is expected far away from the edges (on scale L). However, in recent experiments on low-symmetry samples, Sih *et al.*¹⁰ observed polarized spins away from the edges of a GaAs sample subjected to an electric current and concluded that there are transport effects beyond the simplest spin Hall effect near edges.

In existing analytical theories of the spin Hall effect, spin polarization in spin-orbit coupled media has been considered in the linear transport regime for small electric field \mathbf{E} . Here we show that in this regime, spin generation away from boundaries is forbidden or strongly suppressed for sufficiently symmetric samples. However, in the context of extrinsic effects, by considering nonlinearities in charge transport, we find a new mechanism of generating electron spins by electric current. This nonlinear regime is of practical importance, because experiments are often performed in a range of electric fields with nonlinear current-voltage characteristics.^{3,11} We then present an analytically solvable model in which the bulk spin generation in a radially symmetric sample geometry is due the nonlinearity and the anisotropy of conductivity tensor. Finally, we numerically solve the charge transport and spin drift-diffusion equations for the sample geometries used in Ref. 10. The patterns of spin accumulation we find strongly resemble experimental findings. We establish the existence of two contributions to the spin polarization: the first contribution is generated at the boundaries and then drifts large distances (while diffusing further away from the boundaries), and the second one is generated away from boundaries. While we find that in the recent experiments the first of these dominated, we propose setups that should allow unambiguous observation of the spins generated in the bulk.

We consider a diffusive system with a weak extrinsic spin-orbit coupling and typical system size L . The spin current contains drift and diffusion contributions. Additionally, electrical current, via the extrinsic spin-orbit coupling, induces a spin Hall current \mathbf{j}_{SH}^z , which acts as a source for the spin polarization $s_z(\mathbf{r})$ with a generation rate $\Gamma_z = -\text{div } \mathbf{j}_{\text{SH}}^z$. For length scales much larger than the mean free path ℓ , spin-orbit processes (e.g., Dyakonov-Perel or Elliot-Yafet mechanisms) lead to a finite spin lifetime τ_s . Together with a spin diffusion coefficient D_s , the spin lifetime defines a spin diffusion length $L_s = \sqrt{D_s \tau_s}$. To analyze the spin polarization away from boundaries, we consider the regime $\ell \ll L_s < L$. On length scales large compared to ℓ and in the absence of an external magnetic field, the spin density $s_z(\mathbf{r})$ obeys the drift-diffusion equation

$$\dot{s}_z = \text{div } (D_s \nabla s_z) - \text{div } (\mathbf{v}_{\text{dr}} s_z) + \Gamma_z - \frac{s_z}{\tau_s}, \quad (1)$$

where drift velocity \mathbf{v}_{dr} is proportional to the local electric current density. This introduces yet another length scale, the drift length $L_{\text{dr}} = v_{\text{dr}} \tau_s$.

In the linear transport regime, one can evaluate Γ_z by writing the spin current induced by the electric field as $\mathbf{j}_{\text{SH}}^z = \hat{\sigma}^{\text{SH}} \mathbf{E}$, with the spin Hall conductivity tensor $\hat{\sigma}^{\text{SH}}$ that does not depend on \mathbf{E} . Assuming noninteracting electrons, in the absence of the intrinsic spin-orbit coupling, one can independently consider the spin species with opposite polarization and then relate the spin Hall effect to the anomalous Hall effect.⁷ In particular, at magnetic field $B = 0$, we find $d\hat{\sigma}^{\text{SH}}/d\varepsilon_F = (\hbar/2\mu e) d\hat{\sigma}^{\text{AH}}/dB|_{B=0}$, with $\hat{\sigma}^{\text{AH}} = \frac{1}{2} [\hat{\sigma}(B) - \hat{\sigma}(-B)]$, and where $\hat{\sigma}(B)$ is magnetic field-dependent charge conductivity, ε_F is the Fermi energy, μ is the magnetic moment, and e is the electron charge. From the Onsager relation for $\hat{\sigma}(B)$, we see that $\hat{\sigma}^{\text{SH}}$ must be anti-symmetric. Using this property for a homogeneous two- or three-dimensional system, we find

$$\Gamma_z = -\frac{1}{2} \sum_{ijk} \sigma_{ij}^{\text{SH}} \epsilon_{ijk} (\nabla \times \mathbf{E})_k = 0, \quad (2)$$

i.e., the spin generation rate vanishes and no spin polarization would be found far away from boundaries in the linear regime.

For a system with intrinsic spin-orbit interaction, the interpretation of the spin currents defined above becomes less clear.^{9,13} Thus, instead we consider the electrically induced spin density $\mathbf{s}(\mathbf{r})$ inside the sample on length scales larger than L_s . For typical sample dimension $L > L_s$, the field \mathbf{E} changes slowly over L_s , and we make a gradient expansion linear in E , leading to $s_i(\mathbf{r}) \approx \sum_j A_{ij} E_j(\mathbf{r}) + \sum_{jk} B_{ijk} \partial_j E_k(\mathbf{r})$. For GaAs, the cubic symmetry group T_d contains mirror planes, implying that \mathbf{s} transforms as a pseudo-vector; thus all A_{ij} vanish. The only pseudo-vector linear in ∇ and \mathbf{E} is $\nabla \times \mathbf{E} = 0$. Going to the next order in the gradient expansion, there are contributions $\propto (\partial_{xx}^2 - \partial_{yy}^2) E_z$ and $\propto \partial_z(\partial_x E_x - \partial_y E_y)$, where x, y, z are the principal crystallographic axes. These terms also vanish in the in-plane geometry ($\partial_z E_i = 0$) with an in-plane electric field ($E_z = 0$).

We have found that spin generation away from boundaries may be forbidden or strongly suppressed in the linear transport regime. Therefore, we will now discuss how nonlinear effects can lead to such spin generation. We will restrict ourselves to the case of extrinsic spin currents that are generated by spin-dependent impurity scattering; they are given by $\mathbf{j}_{\text{SH}}^z = \hat{\mathbf{z}} \times (\frac{\gamma}{2e} \mathbf{J}_c - 2\lambda n \frac{e}{\hbar} \mathbf{E})$,⁷ where the two terms correspond to the skew-scattering and side-jump contributions, respectively. Here, $\mathbf{J}_c = \hat{\sigma} \mathbf{E}$ is the charge current, but now we allow the conductivity tensor to be a function of the electric field. Further, λ is a material-dependent spin-orbit coupling constant and the skewness γ is of order λ but it also depends on the properties of scatterers and on electron distribution function. The side-jump part of the current does not contribute to Γ_z , and we obtain

$$\Gamma_z = \frac{1}{2e} (\nabla \times \gamma \hat{\sigma} \mathbf{E})_z. \quad (3)$$

Assuming that γ is constant, that the conductivity is isotropic, and that its position dependence is described by the local electric field, $\hat{\sigma}(\mathbf{r}) = \sigma(E(\mathbf{r}))$, Eq. (3) simplifies to

$$\Gamma_z = \frac{\gamma}{2e} \frac{d\sigma}{dE} (\nabla E \times \mathbf{E})_z. \quad (4)$$

In samples where the extrinsic spin Hall effect was observed^{3,10} the charge conductivity $\sigma(E)$ was found to be an increasing function of field;^{3,11} we expect that Γ_z is finite in these samples, and spin polarization can be generated away from boundaries (see discussion below).

Next, we show how an *anisotropic*, nonlinear conductivity leads to spin generation away from the boundaries. In general, according to Eq. (3), inhomogeneous electric fields are required for a finite Γ_z . Thus, we now analyze the inhomogeneous field in a Corbino geometry, where a total current I is injected at $r = a$ into an infinite two-dimensional sample. In a (001) film of crystal of full cubic symmetry, the leading nonlinearities in $\mathbf{J}_c(\mathbf{E})$ are

$$J_c^i = (\sigma + \sigma_2 E^2) E_i + \sigma_1 E_i^3, \quad (5)$$

where the components $i = x, y$ are taken along the principal crystal axes and we assume that $\sigma_{1,2} E^2(a) \ll \sigma$. One can expect anisotropic nonlinear terms of considerable magnitude for many-valley semiconductors like SiGe quantum wells, and also for $\text{Al}_x\text{Ga}_{1-x}\text{As}$ quantum wells with x close to the direct-indirect gap transition. We first solve for the electrostatic potential $\Phi(\mathbf{r})$; in polar coordinates it will be of the form $\sum_m \Phi_m(r) \cos 4m\varphi$. The term $\Phi_0(r)$ will not contribute to Γ_z [Eq. (3)], so we next consider the lowest harmonic, $\Phi_1(r) \cos 4\varphi$. Because $\text{div } \mathbf{J}_c = 0$, we see that

$$\frac{d^2 \Phi_1(r)}{dr^2} + \frac{1}{r} \frac{d\Phi_1(r)}{dr} - \frac{16}{r^2} \Phi_1(r) + \frac{3\sigma_1}{2\sigma r^4} \left(\frac{I}{2\pi\sigma} \right)^3 = 0. \quad (6)$$

Requiring that $\Phi_1(r \rightarrow \infty) = 0$, we obtain

$$\Phi_1(r) = \frac{\sigma_1}{8r^2} \left(\frac{I}{2\pi\sigma} \right)^3. \quad (7)$$

The spin generation rate is then

$$\Gamma_z(r, \varphi) = \frac{3\gamma}{4e} \sigma_1 \left(\frac{I}{2\pi\sigma} \right)^3 \frac{\sin 4\varphi}{r^4}. \quad (8)$$

So indeed, the combined anisotropy and nonlinearity of conductivity lead to a spin generation, which, for $r \gg L_s$, results in the spin density is $s_z(r, \varphi) = \Gamma_z(r, \varphi) \tau_s \propto I^3 \sin(4\varphi) / r^4$. We emphasize that this polarization falls off only as a power law. Furthermore, it consists of four sectors of up-spins separated by four sectors of down-spins.

We now analyze the spin polarization $s_z(\mathbf{r})$ in systems with *isotropic* (nonlinear) conductivity but with less symmetric geometries. We consider experiments on unstrained GaAs samples by Sih *et al.*¹⁰ The spin Hall effect in such samples is believed to be primarily extrinsic in origin.^{3,7,8} In these experiments a T-shaped geometry, as shown in Fig. 1, was used. In an electric field, electrons flow from the bottom to the top of the main channel, some of them entering into the side-arm; the gradient of the electrical field $E(\mathbf{r})$ becomes large in the region near the entrance of the arm, and a field-dependent conductivity will then lead to spin generation across this region. Furthermore, due to the spin Hall effect, spins are also generated near the sample edges and can then diffuse and drift along the electric field into the center of the side arm—below, we find that this latter mechanism dominates the experimental observations. We choose realistic values of the parameters as follows. Electron density $n = 3 \times 10^{16} \text{ cm}^{-3}$ and sample dimensions are taken from Ref. 10. Further, we assume that the sample is homogeneous and the spatial dependence of σ , τ_s , and D_s is controlled by the local field $E(\mathbf{r})$. Low field conductivity $\sigma(E)$ for GaAs samples was obtained from unpublished data,¹¹ and for higher fields we took the E -dependence of the conductivity measured for $\text{In}_{0.07}\text{Ga}_{0.93}\text{As}$ in Ref. 3 as a guideline, which increased by a factor of two when

the field increased from 0 to 20 mV/ μm . The spin relaxation time $\tau_s(E)$ was loosely based on the experimental data taken at two points away from the boundaries for a range of electric fields;¹¹ we show our assumed $\sigma(E)$ and $\tau_s(E)$ in Fig. 1(c). Furthermore, it was found in Ref. 3 that the spin diffusion length L_s was field-independent within error bars; thus we take $D_s(E) = L_s^2/\tau_s(E)$ with constant L_s . We chose $L_s = 7 \mu\text{m}$ found from the best fit to the data of Ref. 10 for the main channel. Finally, we take spin-orbit coupling constant $\lambda = 5.3 \text{ \AA}^2$ and estimate the skewness $\gamma = 1/700$.^{7,12} In our simulation, we first solve for the electrostatic potential $\Phi(\mathbf{r})$ for an applied dc voltage and determine the spin generation rate $\Gamma_z(\mathbf{r})$ [Eq. (3)] and the drift velocity $\mathbf{v}_{\text{dr}}(\mathbf{r}) = \mathbf{J}_c(\mathbf{r})/ne$. Because there are no direct indications of a considerable spin relaxation at the boundaries, we consider the spin-conservation boundary condition $\hat{\mathbf{n}} \cdot (D_s \nabla s_z - \mathbf{j}_{\text{SH}}^z) = 0$. This accounts for the spin generated at the boundaries due to the spin Hall effect. We then solve the spin drift-diffusion equation [Eq. (1)] and find the stationary spin polarization $s_z(\mathbf{r})$.

The simulated $s_z(\mathbf{r})$ is shown in Fig. 1(a), taking experimental values for sample dimensions and electric field.¹⁰ The most striking feature is a spin distribution inside the side-arm: it results from spins generated at the boundaries near the corner of the lower part of the side-arm, which diffuse and then drift a distance $L_{\text{dr}} = v_{\text{dr}}\tau_s$, which is much longer than L_s . Conversely, near the upper part of the side-arm the spin population is very low, since spins generated at the boundary drift out of the side-arm; i.e., the strong drift ($L_{\text{dr}} > L_s$) leads to an asymmetric spin distribution. However, in Ref. 10 a square wave voltage V was applied for lock-in detection; then the measured spin polarization, $\frac{1}{2}[s_z(V) - s_z(-V)]$, becomes symmetric, and we show the 'symmetrized' polarization in Fig. 1(b). We find good agreement with experimental data, see Fig. 1(c) in Ref. 10: in particular, the maximum of spin distribution is at a similar position inside the side-arm, about 10 - 15 μm deep. In Fig. 1(c), we show s_z along the central section of the side-arm for different depths of the side-arm and find that for depths of 10 or 20 μm , the spin population is maximal at the right edge of the arm.

The simulation includes contributions from spins generated away from boundaries with rate Γ_z [Eq. (3)]. For comparison, we show the spin polarization for $\Gamma_z = 0$, see dashed line in Fig. 1(c). We, however, find that the absence of Γ_z changes the resulting spin polarization by less than 15%. Therefore, in the parameter regime of the experiments of Ref. 10, the dominant contribution to the stationary spin distribution inside the side-arm comes from the drift of the spins generated at the sample boundaries. This results from the large drift distance L_{dr} , which is of the same length scale as the width of the side-arm.

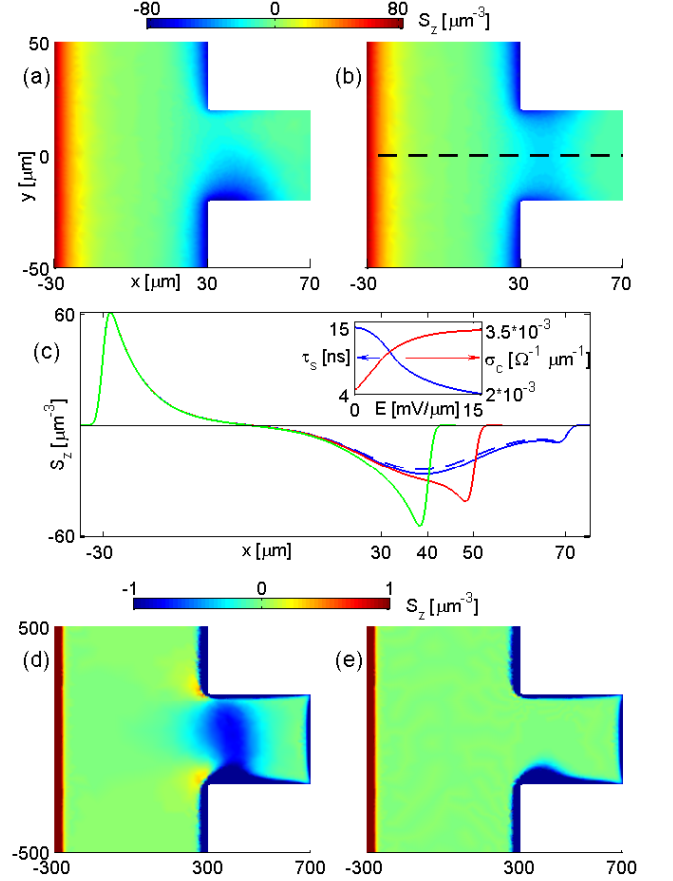


Figure 1: Simulated spin accumulation $s_z(\mathbf{r})$ for experimental geometry and parameters of Ref. 10. Electron flow is from bottom to top in the main channel, and spills over into the side-arm. Distances are measured in microns and electric field in the main channel is 9.5 mV/ μm . (a) Numerical solution of spin drift-diffusion equation [Eq. (1)] for a 40 μm sidearm in the dc regime. (b) Symmetrized spin accumulation $\frac{1}{2}[s_z(V) - s_z(-V)]$. (c) Spin polarization $s_z(x, y)$ (convoluted with a Gaussian with standard deviation of 1 μm that is associated with laser spot) for $y = 0$ (along dashed line in (b)) and for side-arms of depth 10 (green), 20 (red), and 40 μm (blue) is in good agreement with the experimental data in Fig. 1c of Ref. 10. The dashed line shows a simulation without bulk spin generation ($\Gamma_z = 0$). The inset shows spin relaxation time $\tau_s(E)$ and charge conductivity $\sigma(E)$ as used in our simulation. Panels (d), (e) show $s_z(\mathbf{r})$ on a different color scale for a sample larger by a factor $\alpha = 10$. In (e), the spin generation rate Γ_z is neglected.

In order to distinguish spins generated in the bulk from those originating at the boundaries, one needs a set up where both L_s and L_{dr} are smaller than the width of the side arm, L . While $L_s < L$ was satisfied in the experiments of Ref. 10 and in the simulations above, $L_{\text{dr}} < L$ was not. The inequality can be achieved (i) by reducing L_{dr} with a smaller applied field (and, therefore, smaller drift velocity), (ii) by reducing L_{dr} by pulsing the ap-

plied fields and thus allowing drift only for a shorter time, (iii) by using an alternating sequence of pulsed electric fields, which can largely cancel the drift and the spin generation at the boundaries, or (iv) by increasing sample dimensions L . This exponentially suppresses the contributions from the boundaries (as long as L_s is sufficiently short), making the relative contribution of the generation away from boundaries arbitrarily large. However, this also suppresses the absolute value of spin polarization, as we discuss now.

For approach (i), a smaller drift velocity is achieved by choosing a sufficiently small electric field, so that $v_{dr} \ll L/\tau_s$. Because of the scaling $\Gamma_z \propto \sigma'(E)E^2/L$, with $\sigma'(E) = d\sigma/dE$, small drift velocities also imply that spin polarization due to generation away from boundaries is weak. (ii) When the electric field is only applied for pulses of duration t_p , which are short compared to τ_s , the drift length is reduced to $L_{dr} = t_p v_{dr}$. Also, the pulses must be at least τ_s apart, thus the average spin polarization signal is reduced from the dc case by a factor smaller than t_p/τ_s . For example, applying electric field pulses with $t_p = 1$ ns and separation time 20 ns, for the parameters used in Fig. 1, spin generation away from boundaries could be observed with a time-averaged value of $s_z \lesssim 0.2 \mu\text{m}^{-3}$. Another approach (iii) is to use alternating pulses of large positive E for duration t_1 and negative E of smaller magnitude for a longer time t_2 , such that the time-averaged electric current is zero. Then, if the period $t_1 + t_2$ is smaller than both τ_s and L/v_{dr} , the effects of spin drift should be largely canceled. Furthermore, during t_1 and t_2 equal amounts of spin polarization are generated at the boundary, but with opposite signs, which leads to a cancellation of the contribution of spins generated at the boundaries. In contrast, because the bulk spin generation Γ_z is nonlinear, it can have a nonzero time average. Thus, the effectiveness of this scheme will depend on the strength of nonlinearities involved.

Note that in approaches (i)-(iii), diffusion of spins generated at the boundaries may still dominate $s_z(\mathbf{r})$ in the bulk. For example, in simulations with the geometry of Fig. 1 but for smaller fields, the bulk s_z still contains a large relative contribution from spins generated at the boundaries. To eliminate such a diffusion effect, one could use approach (ii) in a pump-probe scheme, where the spin polarization is detected shortly after the pulse, providing a direct measurement of $\Gamma_z(\mathbf{r})$.

The most straightforward way to reveal spin generation away from boundaries is to increase the sample's linear dimensions by a factor α big enough so that the sidearm opening exceeds the drift length L_{dr} , while keeping the

average electric field in the main channel fixed (iv). This reduces Γ_z and hence the bulk spin polarization by a factor α . However, the signal to noise should not decrease since the signal can be taken from an area that is larger by a factor of α^2 , thus reducing the noise by α . Figs. 1(d,e) demonstrate spin populations in a sample 10 times bigger than the sample of Fig. 1. A noteworthy feature is found in the vicinity of the corners: the spin population there is of the opposite sign than the population on the adjacent boundary. This is a distinctive feature of spin generation away from boundaries. For comparison, we show in Fig. 1(e) the spin polarization for $\Gamma_z = 0$. No spin polarization is found in the central part of the sidearm; therefore, the spin polarization in the central part of Fig. 1(d) indeed results from spins generated away from boundaries.

In conclusion, we have shown that, in a linear transport regime, the generation of spin polarization away from boundaries is forbidden or strongly suppressed. However, in nonlinear transport, spins can be generated away from boundaries and we analyze such generation resulting from spin Hall currents due to the “extrinsic” skew scattering mechanism. For an anisotropic nonlinear charge conductivity tensor, we analytically evaluate the spin generation in a Corbino geometry. We also simulate the spin polarization in a T-shaped geometry using isotropic nonlinear conductivity and field-dependent spin lifetimes, appropriate to recent experiments. We find that the spin accumulations in the experiments of Ref. 10 were primarily due to drift of spins generated at the boundaries, but we suggest other setups, where drift should be relatively unimportant, and nonlinear spin generation away from boundaries should be observable.

We thank D.D. Awschalom for helpful discussions and for providing us with unpublished data. This work was supported in part by NSF grants DMR05-41988 and PHY01-17795, and by Harvard Center for Nanoscale Systems.

Note Added: In a recent work, Stern *et al.*^{11,14} have independently shown that drift alone can account for observations of Ref. 10. Golizadeh-Mojarad and Datta¹⁵ have obtained spin polarizations qualitatively similar to those seen in experiments¹⁰ using a model with intrinsic (Rashba) spin orbit coupling. However, the spin coherence length and sample dimensions used were two orders of magnitude smaller than the experimental values. Pershin and Di Ventra¹⁶ considered rectangular samples with inhomogeneous charge density n , which leads to spin generation linear in the electric field, assuming that $\sigma \propto n$ [cf. Eq. (3)].

¹ M.I. Dyakonov and V.I. Perel, Phys. Lett. **35A**, 459 (1971).

² J.E. Hirsch, Phys. Rev. Lett. **83**, 1834 (1999).

³ Y.K. Kato, R.C. Myers, A.C. Gossard, and D.D.

Awschalom, Science **306**, 1910 (2004).

⁴ S. Murakami, N. Nagaosa, and S.-C. Zhang, Science, **301**, 1348 (2003).

⁵ J. Sinova, D. Culcer, Q. Niu, N.A. Sinitsyn, T. Jungwirth,

- and A.H. MacDonald, Phys. Rev. Lett., **92**, 126603 (2004).
- ⁶ J. Wunderlich, B. Kaestner, J. Sinova, and T. Jungwirth, Phys. Rev. Lett. **94**, 047204 (2005).
- ⁷ H.-A. Engel, B.I. Halperin, and E.I. Rashba, Phys. Rev. Lett. **95**, 166605 (2005).
- ⁸ W.-K. Tse and S. Das Sarma, Phys. Rev. Lett. **96**, 056601 (2006).
- ⁹ For theory reviews, see H.-A. Engel, E.I. Rashba, and B.I. Halperin, cond-mat/0603306; J. Schliemann, Int. J. Mod. Phys. B **20**, 1015 (2006) and references therein.
- ¹⁰ V. Sih, W.H. Lau, R.C. Myers, V.R. Horowitz, A.C. Gosard, and D.D. Awschalom, Phys. Rev. Lett. **97**, 096605 (2006).
- ¹¹ D.D. Awschalom (private communication).
- ¹² This value of γ is found from a corrected numerical evaluation, following Ref. 7.
- ¹³ J. Shi, P. Zhang, D. Xiao, and Q. Niu, Phys. Rev. Lett. **96**, 076604 (2006).
- ¹⁴ N.P. Stern *et al.* (in preparation, to be submitted to Appl. Phys. Lett.)
- ¹⁵ R. Golizadeh-Mojarad and S. Datta, cond-mat/0703280.
- ¹⁶ Y. Pershin and M. Di Ventra, cond-mat/0703310.